ECS Transactions, 68 (1) 1609-1616 (2015)
10.1149/06801.1609ecst ©The Electrochemical Society

Fabrication of $Mn_{1.5}Co_{1.5}O_4$ by Electrostatic Spray Deposition for Application as Protective Coating on Alloy Interconnects for Solid Oxide Fuel Cells

Leandro da Conceição[a,b,c], Elisabeth Djurado[a,b], Laurent Dessemond[a,b,] E. N. S. Muccillo[c]

[a]Univ. Grenoble Alpes, CNRS, LEPMI, F-38000 Grenoble, France
[b]Univ. Grenoble Alpes CNRS, SIMAP, F-38000 Grenoble, France
[c]Energy and Nuclear Research Institute–IPEN
P.O. Box 11049, S. Paulo, 05422-970, SP, Brazil

A $Mn_{1.5}Co_{1.5}O_4$ (MCO) protective coating was deposited by Electrostatic Spray Deposition on the SS446 alloy used as interconnects in Solid Oxide Fuel Cells. The main purpose of this work was to verify the feasibility this technique to inhibit the Cr volatilization and the subsequent SOFC cathode poisoning. Phase crystallization was obtained by thermal annealing at 800 °C in air, after deposition. The corrosion resistance behavior of the uncoated and coated steels was investigated by electric and thermogravimetric measurements. The coated films, 400 nm thick, were found efficient in reducing the oxidation rate, by limiting the outward Cr^{3+} diffusion. The area specific resistance of the coated SS446 alloy was found to be much lower (6.7 $m\Omega.cm^2$) and more stable as compared to the uncoated one (80 $m\Omega.cm^2$), after oxidation for 200 h at 800 °C in ambient air. These results evidence the good performance of the deposition technique for fabricating thin, crack free and dense conductive $Mn_{1.5}Co_{1.5}O_4$ coatings on ferritic alloys.

Introduction

Chromium containing alloys used as interconnects in Solid Oxide Fuel Cells (SOFCs) exhibit a number of advantages over ceramic interconnects, such as enhanced mechanical strength, lower cost and superior seal efficiency in stacks (1, 2). The main concern about this type of material is the chromium cathode poisoning resulting from a high volatility of Cr(VI) oxides, like CrO_3 and $CrO_2(OH)_2$, outgassing from the oxidized alloy surface (1-4).

Previous studies have revealed that application of a spinel like protective coating may reduce the chromium volatilization by, first, acting as a barrier for Cr migration (4-6), and, secondly, by reducing the oxidation rate of the alloy via addition of reactive elements in the coatings (7). Referring to their electrical conductivity and thermal expansion characteristics, the promising spinel candidates for coatings on ferritic alloys are Co_3O_4, $CuFe_2O_4$, $(Mn,Co)O_4$, $(Mn,Cu)_3O_4$ (8) and (Mn,Co,Fe_3O_4) (9). Experimentally, a $(Mn,Co)_3O_4$ (MCO) layer has been shown to be an effective barrier against Cr outward transport (10).

Different deposition methods have been exploited to prepare MCO coatings on ferritic interconnects, such as slurry deposition (11), physical vapor deposition (12), electrophoretic deposition (13), and more recently, thermal co-evaporation (14). To obtain an effective coating of practical interest, some physical characteristics such as adherence, density, crack formation/inhibition and thickness as to be considered. A few studies have been devoted to the influence of the thickness and the morphology of the coating on chromium diffusion. As a negative example, the deposition of a protective layer of $MnCo_0O_4$ by slurry coating (~15 µm thick) on a Crofer 22APU, was shown to result in the same oxidation rate than that of an uncoated alloy at 900°C in wet air (15). This was related to an insufficiently tight microstructure, and to a higher electrical conductivity of the spinel phase formed in the presence of $MnCo_2O_4$.

The electrostatic spray deposition (ESD) method is capable of giving improved properties to various films prepared for several applications (16-18). ESD has several advantages such as the use of a simple set-up and inexpensive and nontoxic precursors, the high deposition efficiency, direct deposition under ambient atmosphere and easy control of the layer morphology.

In a previous work, the authors utilized this method to prepare thin (300 nm thick) films of lanthanum manganite (LSM) on SS446 alloy with excellent adhesion and high density (17).

The main purpose of this work was to investigate the effectiveness of the ESD method to fabricate thin, crack free and dense $Mn_{1.5}Co_{1.5}O_4$ coatings on SS446 ferritic steel. We also evaluate the film efficiency for inhibiting the Cr volatilization from the oxidized SS446 alloy, keeping in mind its application as interconnect in SOFCs.

Experimental Details

$Mn_{1.5}Co_{1.5}O_4$ coatings were performed on disc shaped (ϕ 10 mm, thickness=1 mm) of ferritic stainless steel SS446 (Ugitech, France). A vertical ESD set up described elsewhere (17) was used. The chemical composition of the SS446 alloy is given in Table 1. The chromium content of this ferritic alloy is similar to that of the Crofer 22APU, which has been thoroughly investigated for application as interconnect in SOFCs.

ESD technique is basically a simple three-step process based on electrohydrodynamics laws (17). The first step consists in the creation of an aerosol from a precursor solution, at a needle tip, by applying a high dc voltage between it and the substrate. The second step is the transportation of the aerosol from the needle tip to the substrate surface by the electric field. The third and last step is the formation of the coating resulting from the droplet impact on the substrate surface. The physical characteristics of these steps are key factors for the coating microstructure. The droplet size has to be well controlled versus the other ESD parameters. The precursor solutions with a nominal concentration of 0.02 $mol.L^{-1}$ were prepared by dissolving $Co(NO_3)_2.6H_2O$ and $Mn(NO_3)_3.6H_2O$ in a mixture of ethanol, ETOH (C_2H_5OH, 99.9%) and butyl carbitol, BC ($CH_3(CH_2)_3OCH_2CH_2OCH_2CH_2OH$, 99%) with 67:33 vol.% ratio.

The surface of the substrate was prepared according to the same procedures as those described for LSM films (17). The specific parameters used for the coating were: solution flow rate 0.5 $mL.h^{-1}$, nozzle to substrate distance 25 mm, deposition time 60 min, and substrate temperature 450°C. All the as prepared coatings were amorphous and a subsequent annealing at 800°C for 2 h in ambient air was carried out for crystallization.

The oxidation behavior of both the uncoated and MCO coated SS446 alloys were determined by the weight change at 800 °C, in an air flow rate of 6 $L.h^{-1}$.

Three oxidation tests for each sample were performed and the accuracy of the weight measurements was 0.1 mg, for 250 h in intervals of 50 h with heating and cooling rate of $2°C.min^{-1}$.

Structural characterization was carried out by X-ray diffraction, XRD, with a PANalytical X'Pert Pro MPD diffractometer in the 10-90° 2θ range with $2°.min^{-1}$ steps. The morphology and chemical composition of the films were analyzed by field emission scanning electron microscopy; SEM (Zeiss Ultra 55) coupled to an energy dispersive X-ray analyzer, EDS (Zeiss 1540XB). The area specific resistance (ASR) was recorded as a function of the holding time up to 200 h at 800°C in ambient air by a DC two-point, four wire probe equipment. Platinum meshes were used as current collectors to avoid penetration of the metal electrode through the coating layer. A constant current of 10 mA was applied through Pt probes and monitored with a multimeter (Hewlett Packard 34401A). Further details on electrical measurements may be found in previous works (3,17,19). The ASR measurements were triplicated and the values were observed to remain constant within 10% under each set of experimental conditions.

TABLE I: Chemical composition (in wt.%) of the ferritic SS446 alloy.

Sample	Fe	Cr	Mn	Si	Mo	V	W	Ni	Cu
SS446	Bal.	23.15	0.53	0.36	0.07	0.11	0.02	0.20	0.15

Results and Discussion

Structure and Microstructure

SEM micrographs of the surface and cross-section of MCO-coated SS446 alloy are shown in Fig. 1. A homogeneous microstructure with a narrow distribution of grain size can be observed at the surface of the films (Fig. 1a). The cross-section micrograph (Fig. 1b) reveals a dense, crack-free and homogeneous MCO layer, approximately 400 nm in thickness. The main chemical species detected in the cross section by EDS were Mn and Co along with O (Fig. 1c). A Cr-rich sub-layer might have been formed as suggested by the small Cr peak in the spectrum.

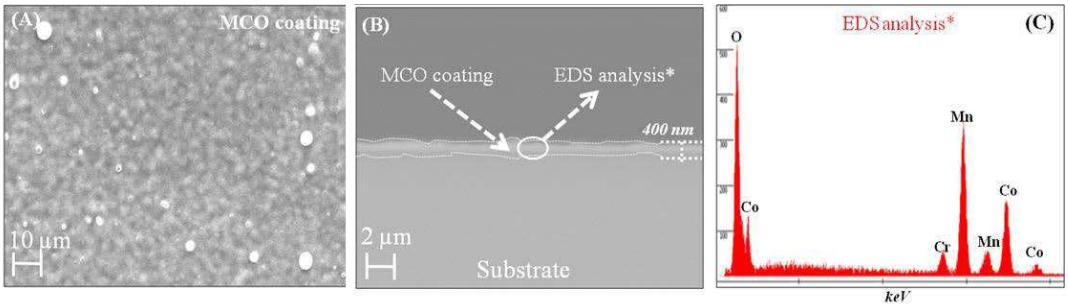

Figure 1. SEM micrographs of (a) surface and (b) cross section, and (c) EDS spectrum of MCO (400 nm thick) coated on the SS446 alloy after annealing at 800°C for 2 h in ambient air.

Fig. 2 shows a SEM micrograph recorded after oxidation at 800°C for 200 h in air. Some cracks are observed on the surface of the MCO. The faceted grains are possibly related to a duplex Cr_2O_3 and/or $(Cr, Mn)_3O_4$ phases (3), as indicated by the EDS analysis (Fig. 1c). No cracks are evidenced on the surface of the coated alloys since the MCO film, 400 nm thick, is present, leading to improved adherence of the film. After 200 hours of oxidation, the thickness of the Cr_2O_3 and/or $(Cr, Mn)_3O_4$ layers remained constant demonstrating the efficiency of the coating as a barrier for Cr diffusion.

Figure 3 depicts the XRD pattern of the MCO coated SS446 alloy after annealing at 800°C for 2 h in ambient air. The main diffraction peaks of the SS446 steel are detected along with several low intensity peaks highlighted in the inset. The spinel coating film with nominal composition $Mn_{1.5}Co_{1.5}O_4$ exhibits a dual phase structure with cubic ($MnCo_2O_4$, ICSD 20-1314) and tetragonal (Mn_2CoO_4, ICSD 39-197) phases similarly to MCO-coated Crofer22APU (14,20). No other phases were detected by XRD.

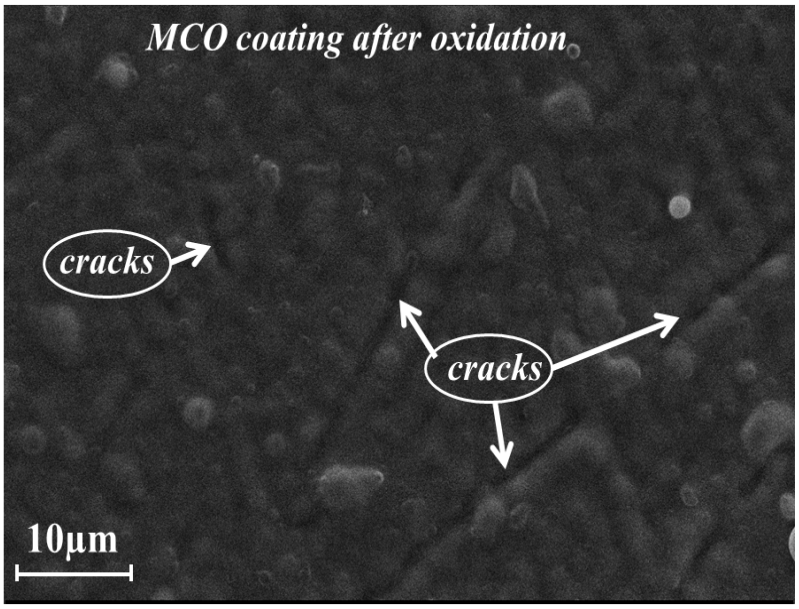

Figure 2. SEM micrograph of MCO (400 nm thick) coated SS446 alloy after oxidation at 800ºC in air atmosphere.

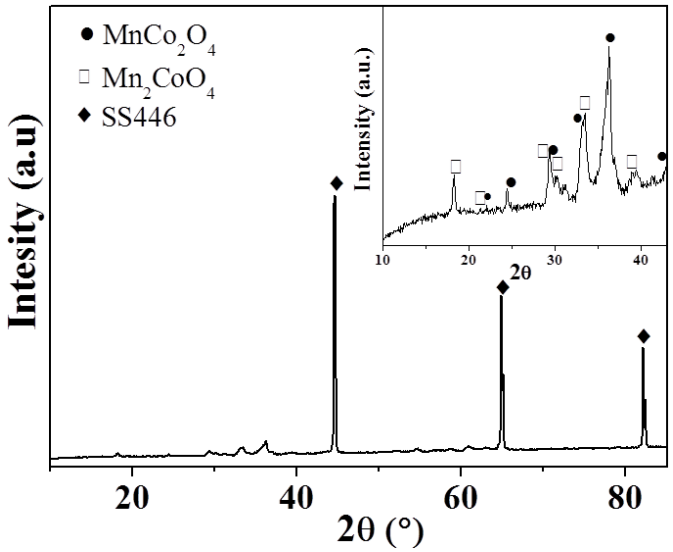

Figure 3. XRD pattern of MCO coated SS446 alloy after annealing at 800°C for 2 h in ambient air. Inset: from t 10 to 45º 2θ range.

Oxidation Behavior

Thermogravimetric analyses were performed on uncoated and MCO-coated SS446 alloy at 800ºC for 250 h in air. The weight gain is an increasing function of temperature with a parabolic oxidation behavior following the equation (1) (21):

$$\left(\frac{\Delta m}{S}\right)^2 = K_p\ t \qquad [1]$$

where Δm (g) is the weight gain, S (cm^2) the total oxidized area, Kp ($g^2\ cm^{-4}\ s^{-1}$) the apparent parabolic rate constant, and t (s) the oxidation time. The parabolic rate law was verified by plotting the ratio of the weight gain to the total oxidized area versus time (Fig. 4). The corresponding slopes enabled to calculate the parabolic rate constant, assuming a diffusion controlled oxidation process (22).

The apparent rate constant Kp is 2.6 10-13 $g^2\ cm^{-4}\ s^{-1}$ for uncoated SS446 alloy. This value is higher than those previously reported (4-8 $10^{-14}\ g^2\ cm^{-4}\ s^{-1}$) for uncoated ferritic stainless steels with chromium content varying between 22 and 25 wt.% without additional alloying elements and for annealing times up to 1200 h in air at 800 ºC (23-27). Yang et al. (21) determined a Kp value of 1.3 $10^{-13}\ g^{-2}\ cm^{-4}\ s^{-1}$ at 800ºC in air, which is close to the value obtained in this work. In coated SS446 alloy the value of the apparent rate constant is 1.5 $10^{-14}\ g^{-2}\ cm^{-4}\ s^{-1}$ after 250 h at 800ºC in agreement with previous results on LSM coating SS446 alloy (17). The performance of oxidation resistance of metallic interconnects was improved as well by applying a similar protective coating based on cobalt-containing spinels (7,23,28,29). The decrease of Kp indicates a partial hindering of the growth of oxide scale on the alloy.

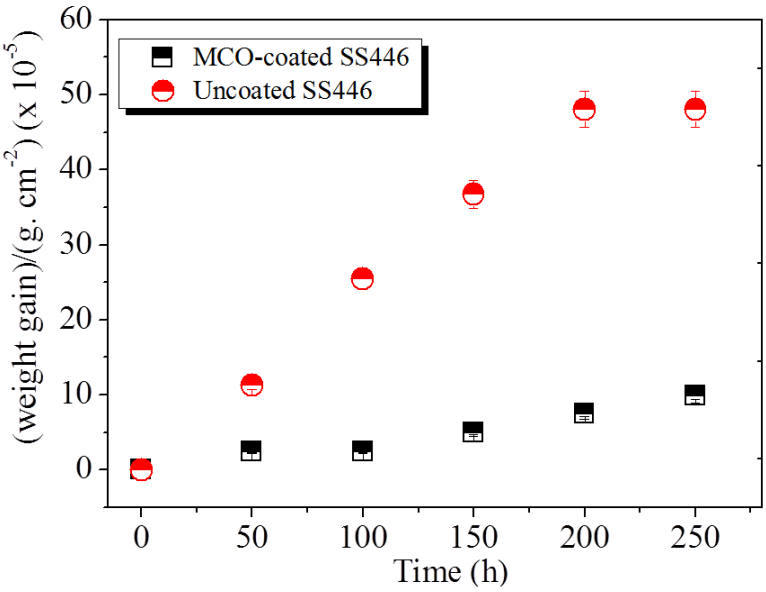

Figure 4. Weight gain during oxidation in air at 800ºC for 250 h of uncoated and MCO coated SS446 alloy.

Area Specific Resistance

The evolution of the ASR for uncoated and MCO coated SS446 alloy versus oxidation time at 800ºC in air is shown in Fig. 5. For the uncoated alloy, the decrease of the ASR during the first 10 h may be due to an enhanced surface contact with the current collector. Indeed, platinum meshes were used as current collectors to avoid diffusion of platinum in the growing oxide scale. For longer aging times, the ASR increases steadily, as already observed for uncoated ferritic steels with similar chromium content (17,30). This ASR increase is likely to be related to the continuous growth of the oxide scale. After 200 h, the ASR of the uncoated alloy is below 80 mΩ cm^2, higher than those reported for other ferritic steels with similar chemical compositions (lower than 40 mΩ cm^2 (20)). This difference may be attributed to the large silicon content of the SS446 steel (Table 1). Adding elements, such as niobium and molybdenum, which lead to the formation of Laves phases could prevent this negative effect of silica, as discussed in (3).

The area specific resistance of MCO coated alloy decreases during the first 50 h of oxidation, as shown in Fig. 5 (inset). We assigned this decrease to interactions between the spinel coating and subjacent layers (by elemental interdiffusion). This effect yields an improved electrical conductivity, compensating the oxide scale growth (31). In the absence of any cracks and spallation of the oxide scale and because of the good adherence of the MCO coating, the recorded increase is likely to be due to the continuing growth of the interfacial oxide of low conductivity. After 50 h of oxidation, the ASR of the coated steel reached 6.7 mΩ cm^2 and then remains constant up to 200 h. It is worth noting that this value is considerably lower than those reported for metallic interconnects coated with spinel phases (6,23,32), and fits well the required limit for application in SOFCs (33). These results evidence the reliability of the ESD technique to prepare protective coatings of $Mn_{1.5}Co_{1.5}O_4$ on metallic interconnects for SOFC application.

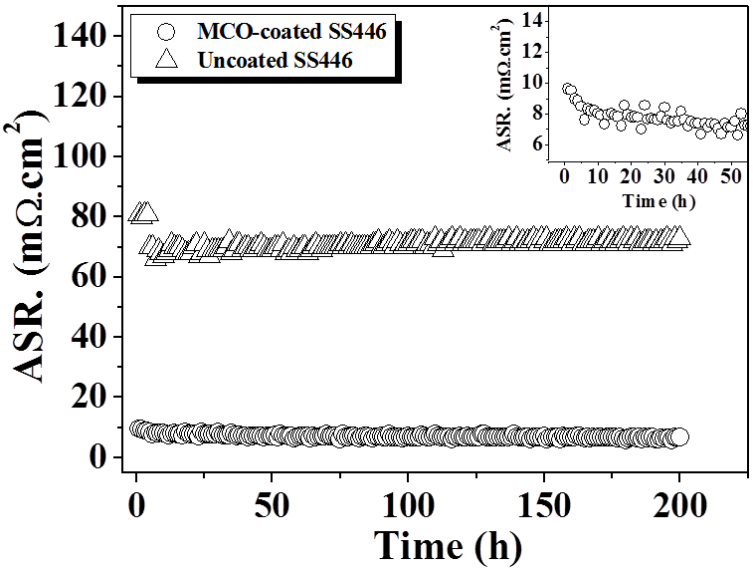

Figure 5. Area specific resistance as a function of the oxidation time at 800ºC in air of 400 nm MCO film coated and uncoated SS446 alloy. Inset: ASR for the first 50 h of the MCO coated ferritic steel.

Conclusion

The results show that the electrostatic spray deposition is an appropriate alternative method for fabricating conductive MCO coatings on SS446 alloys. A careful adjust of the deposition parameters allowed us to obtain an optimized microstructure consisting of a continuous, crack-free and dense layer of $Mn_{1.5}Co_{1.5}O_4$, 400 nm thick. The annealed thin film exhibits a dual phase profile of cubic and tetragonal structures. The parabolic oxidation rate constant estimated for the coated alloy is about one order of magnitude lower than that of the uncoated one. A low value (6.7 mΩ cm^2) of the area specific resistance was obtained for the coated alloy after 200 h at 800 ºC.

Acknowledgements

The authors acknowledge FAPESP for financial support (2011/51689-3 and 2012/07648-3), and Dr. C. Roux for valuable assistance during experiments.

References

1. K. Hilpert, D. Das, M. Miller, J. Electrochem. Soc. **143** (1996).
2. J. Fergus, J. W. Hui, R. Li, X. Wilkinson, D. P. Zhang, Solid Oxide Fuel Cells: Materials, Properties and Performance, CRC Press, Boca Raton, New York, (2009).
3. L. Da Conceição, L. Dessemond, E. Djurado, M. M. V. M. Souza, Int. J. Hydrogen Energy **38** (2013).
4. J. W. Fergus, Mater. Sci. Eng. **A397** p. 271-283 (2005).
5. N. Shaigan, W. Qu, D. G. Ivey, W. Chen, J. Power Sources **195** (2010).

6. X. Montero, F. Tietz, D. Sebold, H. P. Buchkremer, A. Ringuede, M. Cassir, A. Laresgoiti, I. Villarreal, J. Power Sources **184** (2008).
7. X. Chen, P. Hou, C. Jacobson, S. Visco, L. De Jonghe, Solid State Ionics **176** (2005).
8. Z. Yang, G. Xia, Z. Nie, J. Templeton, J. W. Stevenson, Ce-Modified, Solid State Lett. **11** (2008).
9. R. Trebbels, T. Markus, L. Singheiser, J. Electrochem. Soc. **157** (2010).
10. A. Petric, H. Ling, J. Am. Ceram. Soc. **90** (2007).
11. Z. Yang, G. Xia, X. Li, J. Stevenson, Int. J. Hydrogen Energy **32** (2007).
12. A. Balland, P. Gannon, M. Deibert, S. Chevalier, G. Caboche, S. Fontana, Surf. Coatings & Technol. **203** (2009).
13. H. Zhang, Z. Zhan, X. Liu, J. Power Sources **196** (2011).
14. L. C. Ajitdoss, F. Smeacetto, M. Bindi, D. Beretta, M. Salvo, M. Ferraris, Mater. Lett. **95**, (2013).
15. A. H. Persson, L. Mikkelsen, P. V. Hendriksen, M. A. J. Somers, J. Alloy. Compd. **521** (2012).
16. J. L. Shui, Y. Yu, C. H. Chen, Appl. Surf. Sci. **253** (2006).
17. L. da Conceição, L. Dessemond, E. Djurado, E. N. S. Muccillo, Surf. Coatings &Technol. **254** (2014).
18. M. G. Mali, H. Yoon, S. Na, J.-Y. Choi, H. Y. Kim, B. C. Lee, B. N. Kim, J. H. Park, S. S. Al-Deyah, S. S. Yoon, Appl. Surf. Sci. doi: 10.1016/j.apsusc.2014.06.097.
19. L. da Conceição, L. Dessemond, E. Djurado, M. M. V. M. Souza, J. Power Sources **241,** (2013).
20. Z. Yang, G. Xia, S. P. Simner, J. W. Stevenson, J. Electrochem. Soc. **152** (2005).
21. Z. Yang, K. S. Weil, D. M. Paxton, J. W. Stevenson, J. Electrochem. Soc. **150** (2003).
22. P. Jian, L. Jian, H. Bing, G. Xie, J. Power Sources **158**, (2006).
23. N. V. Gravilov, V. V. Ivanov, A. S. Kamenetskikh, A. V. Nikonov, Surf. Coatings Technol. **201**, (2011).
24. X. Montero, F. Tietz, D. Stöver, M. Cassir, I. Villareal, Cor. Sci. **51**, (2009).
25. Z. Yang, G.-G. Xia, G. D. Maupin, J. W. Stevenson, Surf. Coatings & Technol. **201** (2006).
26. D. W. Yun, H. S. Seo, J. H. Yun, J. M. Lee, K. Y. Kim, Int. J. Hydrogen Energy **37** (2012).
27. J. Fontana, R. Amendola, S. Chevalier, P. Piccardo, G. Caboche, M. Voiviani, R. Molins, M. Sennour, J. Power Sources **171**, (2007) .
28. B. Hua, J. Pu, W. Gong, J. Zhang, F. Lu, L. Jian, J. Power Sources **185**, (2008).
29. B. Hua, W. Zhang, J. Wu, J. Pu, B. Chi, L. Jian, J. Power Sources **195**, (2010).
30. X. Montero, N. Jordán, J. Pinón-Abellán, F.Tietz, D. Stöver, M. Cassir, I. Villareal, J. Electrochem. Soc. **156** (2009).
31. Q. Fu, F. Tietz, D. Sebold, E. Wessel, H.-P. Buchkremer, Corr. Sci. **54**, (2012).
32. S. W. Sofie, P. Gannon, V. Gorokhovsky, J. Power Sources **191**, (2009).
33. P. Yang, C.-K. Liu, J.-Y. Wu, W.-J. Shong, R.-Y. Lee, C.-C. Sung, J. Power Sources **213**, (2012).